High Pressure Phase Equilibria of the Related Substances in the Limonene Oxidation in Supercritical CO_2

Marcos L. Corazza,[†] Lúcio C. Filho,[†] Octávio A. C. Antunes,[‡] and Cláudio Dariva*,[§]

Departamento de Engenharia Química, Centro de Tecnologia, Universidade Estadual de Maringá, Bloco D90, Av. Colombo 5790, Maringá, PR 87020-900 Brazil, Instituto de Química, Universidade do Brasil, CT Bloco A, Lab. 641, Rio de Janeiro, RJ 21945-970 Brazil and Departamento de Engenharia de Alimentos, URI-Campus de Erechim, Av. Sete de Setembro, 1621, 99700-000, Erechim-RS, Brazil

The use of supercritical CO_2 ($SCCO_2$) as an alternative solvent in reactional systems has received increased attention nowadays because of its favorable transport properties that can accelerate mass-transfer limited reactions and also because of imposed environmental restrictions. The comprehension of the phase behavior of the reaction mixture is of relevance to determine selectivity and yield of such reactions at high pressures. In this context, the main objective of this work was to investigate the high-pressure phase equilibrium behavior of binary systems formed by CO_2 with the reactant (limonene), the most common solvents (acetonitrile and dichloromethane), and catalysts and the main products (carvone and 1,2-limoneneoxide) of the limonene catalytic oxidation reactions. The experimental data were measured using the static synthetic method with a variable-volume view cell in the temperature range from (313 to 343) K. Experimental data obtained were corrected modeled with the Peng−Robinson equation of state with the classical quadratic mixing rules.

1. Introduction

Supercritical fluid (SCF) technology has received great attention in the application and development of new processes and products.[1,2] For example, they have been used as solvents in chemical reactions,[3−7] chromatographic analysis,[8] polymer processing,[9,10] pharmaceutical and food processing,[9] coal and petroleum processing,[11] and for environmental purposes.[2,9,12]

Supercritical fluids could be useful as an alterative medium for chemical reactions because of their unique properties. Their gaslike transport properties and liquidlike densities can be easily manipulated by changing pressure and temperature.[4] Besides environmental advantages, one additional attractive feature of SCFs as a medium for chemical reactions is that they can lower mass transfer limitations and allow a better control of selectivity and reaction yield. Also it permits us to combine advantageously the reaction, separation, and purification steps.[5,13] In this sense, the natural use of supercritical carbon dioxide ($SCCO_2$) becomes an interesting possibility to replace organic solvents in many chemical reactions, like the catalytic oxidation of monoterpenes.

The limonene oxidation is an alternative route to carvone production compared with extraction from natural products such as caraway seeds.[14] Limonene oxidation is traditionally carried out in an organic solvent media (for example dichloromethane, acetonitrile, and acetone among others), by using Metal(SALEN) as catalyst and iodozilbenzene as oxidant, via a rebound mechanism.[15] The main products obtained in the catalytic oxidation of limonene are epoxides (1,2-limoneneoxide), ketones (mainly carvone), and alcohols (mainly carveol).[16]

To improve the selectivity and yield of this reaction, $SCCO_2$ can be used totally or partially in place of organic solvents. From an engineering point of view, the knowledge of phase equilibrium behavior of the components involved in the reaction system plays an important role in selecting operating regions and process scale-up. In this work, vapor−liquid equilibrium of binary systems formed by the reactant (limonene), organic solvents (acetonitrile and dichloromethane), and products of the limonene oxidation (1,2-limoneneoxide and carvone) with $SCCO_2$ were measured in the temperature range of (313 to 343) K.

The literature presents some experimental data for CO_2 + limonene.[17−21] Gamse and Marr[18] presented a study of the system CO_2−carvone from (303 to 323) K. 1,2-Limoneneoxide constitutes one of the major oxidation products, but there seems to be no experimental phase equilibrium data for this compound with $SCCO_2$. Here, it may be important to notice that, even when using $SCCO_2$ as an alternative medium for the limonene oxidation reaction, it might be necessary the addition of organic solvents at small concentrations (cosolvent). In this context, this work also reports binary phase equilibrium data of acetonitrile and dichloromethane (most common organic solvents used in the reaction at low pressure) with $SCCO_2$. Phase equilibrium information for the system CO_2/acetonitrile has hardly been reported in the literature.[22,23] The results were modeled using the Peng−Robinson equation of state (PR-EOS) with the classical quadratic mixing rule.[24]

2. Materials and Methods

2.1. Materials. *R*-(+)-Limonene (99%, Sigma), *S*-(+) carvone (98%, Aldrich), 1,2-limoneneoxide (99%, Aldrich), dichloromethane (99%, Carlo Erba), and acetonitrile (99%, Jonhson Mattey) were used without further purification. The CO_2 was 99.9% pure (liquid phase, AGA). The critical properties of pure compounds are presented in Table 1. When experimental values were not available in the literature,[25] they were predicted by the Joback group contribution method.[25]

---

* To whom correspondence should be addressed. Fax: +55-54-5209090. Phone: +55-54-5209000. E-mail: cdariva@uricer.edu.br.

[†] Universidade Estadual de Maringá.

[‡] Universidade do Brasil.

[§] URI-Campus de Erechim.

10.1021/je020150k CCC: $25.00

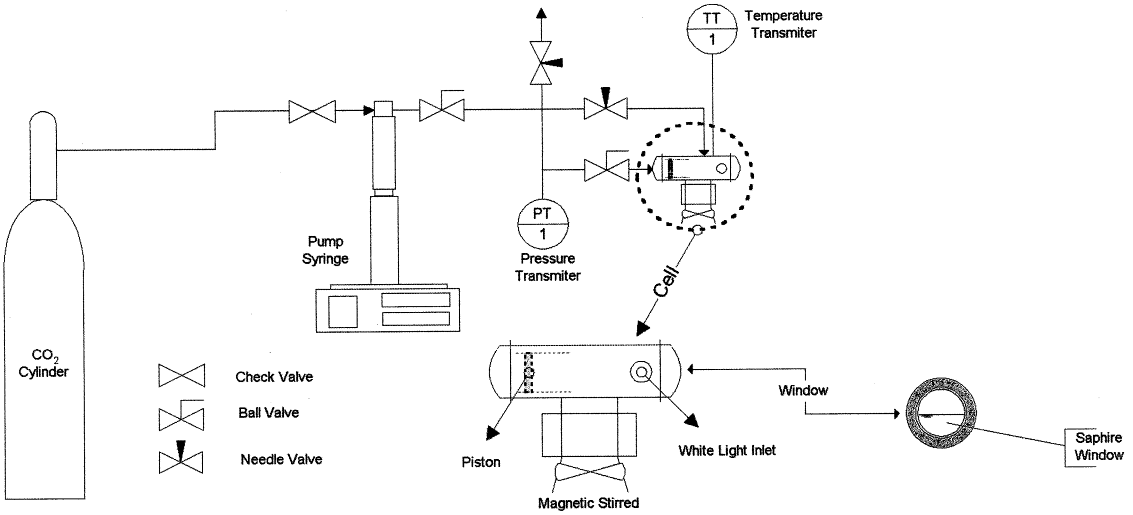

Figure 1. Schematic diagram of the experimental apparatus.

Table 1. Critical Properties and Acentric Factors of Pure Components[25]

compound	MW/(ggmol^{-1})	Tc/K	Pc/MPa	ω
CO_2	44.01	304.21	7.38	0.2236
limonene[a]	136.24	657.16	2.76	0.3396
carvone[a]	150.21	712.76	2.72	0.4930
1,2 limoneneoxide[a]	152.13	661.07	3.05	0.4315
dichloromethane	84.93	510.00	6.30	0.1990
acetonitrile	41.05	547.95	4.83	0.3270

[a] Estimated by Joback group contribution method.

2.2. Apparatus and Procedure. Phase equilibrium experiments (cloud points) were performed in a high-pressure variable-volume view cell. The experimental apparatus used in this work is similar to the one used in previous investigations,[26-29] and thus, only a brief description is given. A schematic diagram of the apparatus is presented in Figure 1, which consists basically of a view cell with two sapphire windows for visual observations, an absolute pressure transducer (Smar LD 301), with an uncertainty of 0.012 MPa, a portable programmer (Smar, HT 201) for the pressure data acquisition and a syringe pump (ISCO 500D). The equilibrium cell has a maximum internal volume of 25 cm^3 and contains a movable piston, which permits the pressure control inside the cell. Phase transitions were recorded visually as bubble or dew points by varying the pressure behind the piston using the syringe pump and CO_2 as the pressurizing fluid. The cell was equipped with an electrical heater and a PID controller (DIGI MEC mark, SHM 112 model). The controller was connected to a thermocouple (PT-100, with an accuracy of 0.1 K), which was in direct contact with the fluid mixture inside the cell body.

Depending on the desired overall composition, an amount of solute was weighed on a high precision scale (Ohaus Analytical Standard, with 0.0001 g accuracy) and loaded into the cell. Then, the cell and all lines were flushed with low-pressure CO_2 to remove residual air. Afterward, the solvent was pumped into the cell in order to reach the preestablished overall composition. The amount of solvent charged was monitored by the change in the volume of the transfer vessel of the pump. Then, the cell content was kept in continuous agitation with the help of a magnetic stirrer and a Teflon-coated stirring bar. After reaching the desired temperature, the cell pressure was increased by applying pressure on the back of the piston with the syringe pump until observation of a single phase. At this point, the system was allowed to stabilize at least 30 min and the cell pressure was decreased slowly until incipient formation of a new phase. The equilibrium pressure was then recorded, after repetition of the experimental procedure at least four times. After completing the measurement at a given temperature, the cell temperature was established at a new value and the experimental procedure was repeated.

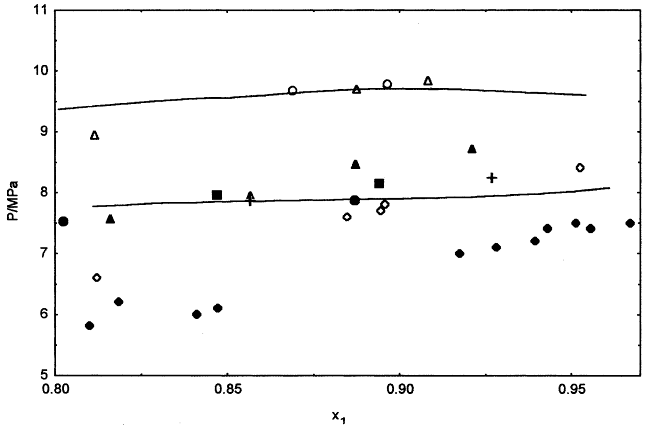

Figure 2. Phase equilibrium diagram for the system CO_2 (1) + limonene (2). Comparison of experimental data measured in this work with the literature. 313 K: +, this work; ▲, Chang and Chen;[19] ■, Akgün et al.;[17] ●, Vieira de Melo et al.;[20] ◆, Gamse and Marr.[18] 323 K: *, this work; △, Chang and Chen;[19] ○, Vieira de Melo et al.;[20] ◇, Gamse and Marr.[18] Lines, PR-EOS.

It is important to mention that, through replicate measurements and the experience with the present apparatus, the uncertainty in pressure values is lower than 0.070 MPa. Concerning the uncertainty in temperature, the arrangement of this work provided a temperature control with a precision better than 0.5 K. With regard to phase composition, the mass of carbon dioxide was carefully accounted for by the volume decay in the syringe pump. It was estimated that the uncertainty was around 0.001 in molar fraction basis.

3. Results and Discussion

To test the reliability of the apparatus and experimental procedure, some tests were performed using the system CO_2 + limonene. This system was chosen because limonene is the reactant of interest in this work and also because the literature is relatively abundant on the experimental data for this system. Figure 2 presents a comparison between the experimental data presented in the literature with those measured in this work at 313 K and 323 K. The

Table 2. VLE Experimental Data for CO$_2$ (1) + Acetonitrile (2)

x_1	P / MPa	σ / MPa	phase transition type	x_1	P / MPa	σ / MPa	phase transition type
			T = 313 K				
0.4919	4.88	0.03	BP	0.8844	7.57	0.02	BP
0.5925	5.64	0.04	BP	0.9426	8.01	0.06	BP
0.7385	6.70	0.02	BP	0.9694	8.10	0.04	BP
			T = 323 K				
0.4919	5.79	0.05	BP	0.8844	9.19	0.05	BP
0.5925	6.68	0.05	BP	0.9426	9.05	0.08	BP
0.7385	8.12	0.03	BP	0.9694	9.02	0.12	DP
			T = 333 K				
0.4919	6.64	0.02	BP	0.8844	10.61	0.04	BP
0.5925	7.78	0.08	BP	0.9426	10.08	0.10	DP
0.7385	9.38	0.03	BP	0.9694	9.93	0.09	DP
			T = 343 K				
0.4919	7.50	0.06	BP	0.8844	11.70	0.03	BP
0.5925	8.84	0.11	BP	0.9426	10.99	0.06	DP
0.7385	10.66	0.05	BP	0.9694	10.61	0.06	DP

Table 3. VLE Experimental Data for CO$_2$ (1) + Dichoromethane (2)

x_1	P / MPa	σ / MPa	phase transition type	x_1	P / MPa	σ / MPa	phase transition type
			T = 313 K				
0.5686	4.65	0.05	BP	0.9301	7.43	0.04	BP
0.6580	5.39	0.06	BP	0.9378	7.62	0.01	BP
0.7437	5.94	0.04	BP	0.9470	7.72	0.03	BP
0.8527	6.81	0.02	BP	0.9727	7.36	0.09	DP
			T = 323 K				
0.5686	5.63	0.02	BP	0.8977	8.69	0.06	BP
0.6580	6.37	0.09	BP	0.9301	8.75	0.05	BP
0.7437	7.04	0.04	BP	0.9378	8.73	0.05	BP
0.8522	8.26	0.07	BP	0.9727	8.30	0.08	DP
			T = 333 K				
0.5686	6.47	0.06	BP	0.8522	9.29	0.03	BP
0.6580	7.30	0.02	BP	0.8977	9.63	0.03	BP
0.7437	8.14	0.03	BP	0.9301	9.26	0.10	DP
			T = 343 K				
0.5686	7.33	0.03	BP	0.8522	10.19	0.06	BP
0.6580	8.38	0.07	BP	0.8977	10.09	0.02	DP
0.7437	9.17	0.05	BP				

Table 4. VLE Experimental Data for CO$_2$ (1) + Carvone (2)

x_1	P / MPa	σ / MPa	phase transition type	x_1	P / MPa	σ / MPa	phase transition type
			T = 313 K				
0.7387	7.76	0.02	BP	0.9663	8.55	0.04	BP
0.8368	8.14	0.02	BP	0.9788	8.58	0.02	BP
0.8979	8.37	0.05	BP	0.9894	8.48	0.08	DP
0.9288	8.48	0.02	BP	0.9954	8.41	0.03	DP
0.9522	8.50	0.01	BP				
			T = 323 K				
0.7387	9.54	0.04	BP	0.9663	10.84	0.05	DP
0.8368	10.36	0.02	BP	0.9788	10.79	0.01	DP
0.8979	11.11	0.02	BP	0.9894	10.82	0.04	DP
0.9288	11.04	0.06	BP	0.9954	10.54	0.04	DP
0.9522	11.05	0.05	BP				
			T = 333 K				
0.7387	11.35	0.04	BP	0.9663	13.21	0.08	DP
0.8368	12.60	0.07	BP	0.9788	12.94	0.04	DP
0.8979	13.44	0.11	BP	0.9894	12.72	0.03	DP
0.9288	13.47	0.04	BP	0.9954	12.05	0.06	DP
0.9522	13.42	0.08	DP				
			T = 343 K				
0.7387	13.34	0.04	BP	0.9663	15.17	0.07	DP
0.8368	14.83	0.02	BP	0.9788	14.66	0.09	DP
0.8979	15.63	0.07	BP	0.9894	14.16	0.06	DP
0.9288	15.59	0.05	DP	0.9954	13.24	0.08	DP
0.9522	15.62	0.04	DP				

Table 5. VLE Experimental Data for CO$_2$ (1) + 1,2-Limoneneoxide (2)

x_1	P / MPa	σ / MPa	phase transition type	x_1	P / MPa	σ / MPa	phase transition type
			T = 313 K				
0.8908	8.29	0.02	BP	0.9790	8.46	0.03	BP
0.9334	8.36	0.03	BP	0.9876	8.43	0.05	BP
0.9751	8.42	0.01	BP	0.9933	8.21	0.03	DP
			T = 323 K				
0.8908	9.98	0.07	BP	0.9790	10.22	0.05	BP
0.9334	10.36	0.03	BP	0.9876	9.72	0.06	DP
0.9751	10.32	0.05	BP	0.9933	9.51	0.08	DP
			T = 333 K				
0.8908	11.86	0.03	BP	0.9790	11.89	0.05	DP
0.9334	12.16	0.04	BP	0.9876	10.90	0.05	DP
0.9751	12.17	0.06	DP	0.9933	10.63	0.11	DP
			T = 343 K				
0.8908	13.76	0.11	BP	0.9790	13.50	0.04	DP
0.9334	13.86	0.03	BP	0.9876	11.84	0.05	DP
0.9751	13.66	0.03	DP				

Table 6. Binary Interaction Parameters of the PR-EOS

system	k_{ij}	l_{ij}
CO$_2$ + limonene	0.0939	−0.0281
CO$_2$ + acetonitrile	0.0864	0.0165
CO$_2$ + dichloromethane	0.0295	−0.0661
CO$_2$ + carvone	0.0556	−0.0499
CO$_2$ + 1,2-limoneneoxide	0.0522	0.0104

present data at both temperatures are in good agreement with the values reported in the literature, except for the data published recently by Gamse and Marr.[18] For the later reference, large divergences are observed. Perhaps, in their case, the pressure drop during the sampling procedure might have led to equilibrium disturbances inside the cell (a fixed volume cell) thus affecting the phase equilibrium composition.[9,30,31] We have also tested our apparatus and experimental procedure at other temperatures (333 K and 343 K), and the results were again in good agreement (deviation always lower than 0.3 MPa) with the literature data.[20]

In Figure 2 are presented the correlation of the experimental data with the PR-EOS with the quadratic mixing rule (two temperature independent adjustable parameters: k_{ij} and l_{ij}). The binary interaction parameters were estimated through the maximum likelihood method coupled to a bubble or dew point algorithm for calculation of VLE according to Asselineau formulation.[32,33] Preliminary tests indicated that the global fitting procedure, instead of isothermal parameter estimation, was adequate to correlate the experimental data. For this system, our results together with the literature data (except those from reference[18]) were used in the regression. Throughout this work, a global parameter regression of the experimental data was accomplished using the PR-EOS leading to the parameter values shown in Table 6.

3.1. CO$_2$ + Organic Solvents Systems. The influence of organic solvents on the reaction yield and selectivity in the catalytic limonene oxidation at low pressures is not well established at present. According to Gomes and Antunes,[15,16] it is possible that the polar solvent can also participate in the stabilization of the catalyst. Thus, the addition of small amounts of organic solvents in the reaction medium might be necessary. In this sense, binary phase equilibrium data between CO$_2$ with the most common organic solvents (acetonitrile and dichloromethane) used in the catalytic limonene oxidation were measured in the temperature range from (313 to 343) K. Table 2 presents the experimental equilibrium values for the system CO$_2$ + acetonitrile, as well as the experimental error and the phase transition type, bubble point (BP), or dew point (DP). In all tables reporting the experimental

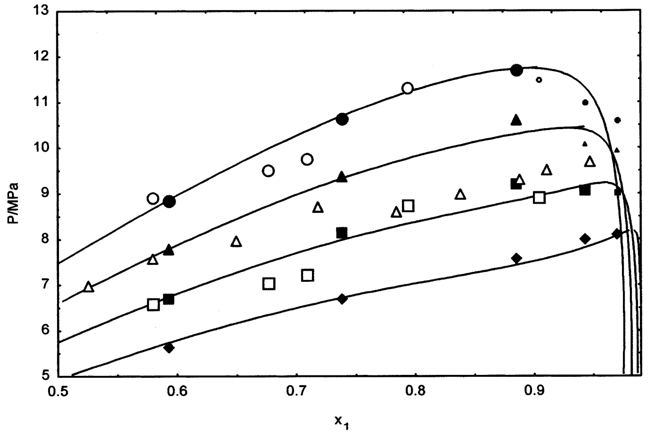

Figure 3. P−x−y diagram for CO_2 (1) + acetonitrile (2) system. ●, BP at 343 K; ●, DP at 343 K; ▲, BP at 333 K; ▲, DP at 333 K; ■, BP at 323 K; ■, DP at 323 K; ◆, BP at 313 K; ○, BP at 343 K, Reighard et al.;[23] ○, DP at 343 K, Reighard et al.;[23] □, DP at 323 K, Reighard et al.;[23] △, DP at 328 K, Byun et al.;[22] Lines, PR-EOS.

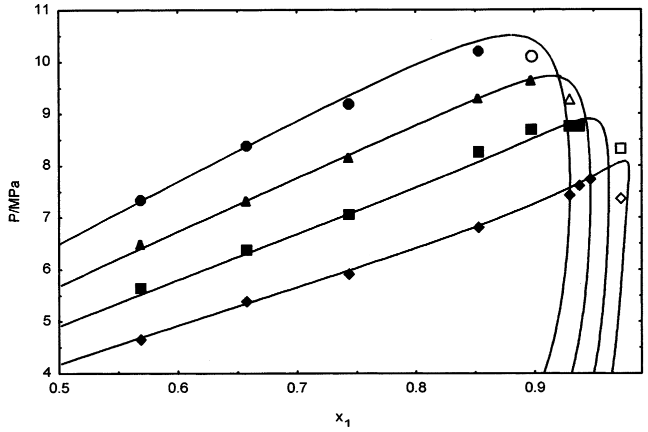

Figure 4. P−x−y diagram for CO_2 (1) + dichloromethane (2) system. ●, BP at 343 K; ○, DP at 343 K; ▲, BP at 333 K; △, DP at 333 K; ■, BP at 323 K; □, DP at 323 K; ◆, BP at 313 K; ◇, DP at 313 K. Lines, PR-EOS.

data, pressure values are in fact average values of at least four replicate runs, and the standard deviations presented reflect experimental errors of these replicates.

Figure 3 gives a comparison between the vapor−liquid equilibrium data for CO_2 + acetonitrile measured in this work and those from the literature.[22,23] Though the temperatures are not the same as that for Byun et al.,[22] one can observe from this figure a reasonable agreement between our results and the literature data. In this figure, it can also be noted some scattering in the data points reported by Reighard et al.,[23] which does not occur for the experimental points obtained in this work. The most data points measured were of bubble point type, for which a small region of the lighter phase appears at the top of the cell. Again, a good representation of the experimental data from the PR-EOS was achieved.

Table 3 presents the experimental results obtained for CO_2 + dichloromethane and Figure 4 shows the calculated and experimental phase boundaries for this system. One can observe that the appearance of a dew point is shifted to lower carbon dioxide compositions with the increase of temperature, indicating the region with a maximum pressure value where the mixture critical point is located.

3.2. CO_2 + Products. The main products of catalytic limonene oxidation are 1,2-limoneneoxide and carvone. For the CO_2 + carvone, there are solubility data[14] obtained from $SCCO_2$ extraction of caraway seeds, making difficult a direct comparison with our data, because it reported the essential oil solubility, a multicomponent mixture, in the fluid phase.

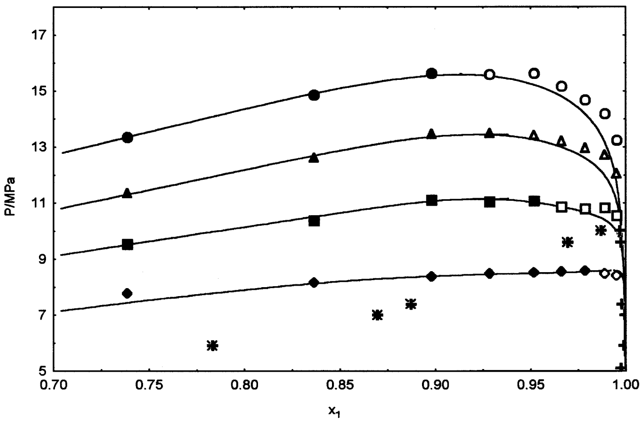

Figure 5. P−x−y diagram for CO_2 (1) + carvone (2) system. ●, BP at 343 K; ○, DP at 343 K; ▲, BP at 333 K; △, DP at 333 K; ■, BP at 323 K; □, DP at 323 K; ◆, BP at 313 K; ◇, DP at 313 K; *, BP at 323 K, Gamse and Marr;[18] +, BP at 323 K, Gamse and Marr;[18] Lines, PR-EOS.

Table 4 presents the experimental results obtained in this work, and Figure 5 shows the P−x-y diagram for CO_2 + carvone. The literature data from Gamse and Marr[18] show lower pressure transitions than the ones measured in this work. For the system CO_2 + limonene, this fact might be attributed to the experimental methodology employed by Gamse and Marr. For the CO_2 + carvone system, bubble and dew point transitions are observed for all temperatures, and as expected, when the temperature is increased, the critical point of the mixture is shifted to lower carbon dioxide compositions. Inspection of Table 4 and Figure 5 reveals that the mixture critical point for this system is, on the basis of carvone composition, around mole fraction 9% at 343 K, 6% at 333 K, 4% at 323 K, and 2% at 313 K.

Table 5 presents bubble and dew point phase transitions for the system CO_2 + 1,2-limoneneoxide and CO_2 + carvone. At similar compositions, the pressure transition values for CO_2 + 1,2-limoneneoxide are slightly lower than for CO_2 + carvone, especially at higher temperatures. This fact may be relevant if we take into account the screening of temperature and pressure regions to perform the limonene oxidation in $SCCO_2$ aiming at a possible separation of the reaction products.

Figure 6 shows the P−x-y diagram for the system CO_2 + 1,2-limoneneoxide, and again, a raise in temperature causes the transition from dew to bubble points (critical region) to be shifted toward lower CO_2 concentrations.

Solubility of Catalyst and Oxidant in $SCCO_2$. First, to check whether the catalyst Ni(SALEN) and the oxidant (iodozilbenzene) may affect the phase behavior of the reactional mixture, some solubility tests in $SCCO_2$ have been carried out at 343 K and pressures up to 25 MPa. We have verified, however, in both cases the presence of a solid phase, indicating that the catalyst and the oxidant present very small solubility in $SCCO_2$.

Additionally, to verify the influence of the catalyst on the phase behavior of the reactional mixture, some comparative tests were carried out. Experimental measurements of phase behavior of the ternary system CO_2 + limonene + small amount of Ni(SALEN) were performed and compared to the CO_2 + limonene system. The results

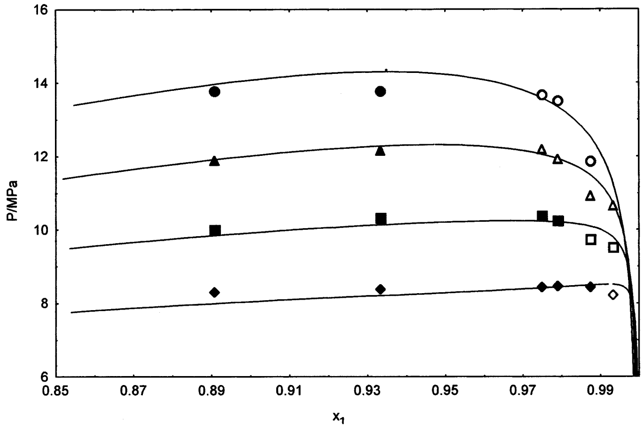

Figure 6. P−x−y diagram for CO_2 (1) + 1,2-limoneneoxide (2) system. ●, BP at 343 K; ○, DP at 343 K; ▲, BP at 333 K; △, DP at 333 K; ■, BP at 323 K; □, DP at 323 K; ◆, BP at 313 K; ◇, DP at 313 K; Lines, PR-EOS.

indicated that the presence of catalyst does not affect significantly the phase behavior of the system, leading to an average pressure decrease lower than 0.30 MPa in all temperatures investigated (313 K to 343 K).

4. Conclusions

In this work, new binary high-pressure phase equilibrium data of CO_2 with the products, reactant, and the most common organic solvents of the catalytic limonene oxidation are reported in the temperature range from (313 to 343) K. Phase transitions, bubble and dew points, were observed when dealing with the products and organic solvents of the reaction. It was observed that the system CO_2−carvone presented pressure transitions slightly higher than the system CO_2 + 1,2-limoneneoxide at similar concentrations, an interesting piece of information that can be useful for a possible fractionation step of the reaction products. It was also observed that the addition of Ni-(SALEN) or iodozilbenze does not affect significantly the phase behavior of the CO_2 + limonene system. The experimental data were modeled with the PR-EOS using the classical quadratic mixing rule providing a good representation of the experimental information.

Literature Cited

(1) Hauthal, W. H. Advances with supercritical fluids [review]. *Chemosphere* **2001**, *43*, 123−135.

(2) Marr, R.; Gamse, T. Use of supercritical fluids for different processes including new developments − a review. *Chem. Eng. Process.* **2000**, *39*, 19−28.

(3) Chateauneuf, J. E.; Nie, K. An investigation of a Friedls-Crafts alkylation reaction in homogeneous supercritical CO_2 and under subcritical and splitphase reaction conditions. *Adv. Environ. Res.* **2000**, *4*, 307−312.

(4) Stradi, B. A.; Kohn, J. P.; Stadtherr, M. A.; Brennecke, J. F. Phase behavior of reactants, products and catalysts involved in the allylic epoxidation of *trans*-2-Hexen-1-ol to (2*R*,3*R*)−(+)-3-Propyloxiranemethanol in high-pressure carbon dioxide. *J. Supercrit. Fluids* **1998**, *12*, 109−122.

(5) Kemmere, M.; Vries, T.; Vorstam, M.; Keurentjes, J. A novel process for the catalytic polymerization of olefins in supercritical carbon dioxide. *Chem. Eng. Sci.* **2001**, *56*, 4197−4204.

(6) Leitner, W. Homogeneous catalysts for application in supercritical carbon dioxide as a “green” solvent. *C. R. Acad. Sci. Paris/Chem.* **2000**, *3*, 595−600.

(7) Franciò, G.; Wittmann, K.; Leitner, W. Highly efficient enantioselective catalysis in supercritical carbon dioxide using the perfluoroalkyl-substituted ligand (*R*,*S*)-3-H_2F_6-binaphos. *J. Organomet. Chem.* **2001**, *621*, 130−142.

(8) Carrilho, E.; Tavares, M. C. H.; Lanças, F. M. Supercritical fluid in analytical chemistry. I. Supercritical fluid chromatography: Thermodynamic definitions. *Quim. Nova* **2001**, *24*, 509−515.

(9) McHugh, M. A.; Krukonis, I. *Supercritical Fluid Extraction: Principles and Practice*, 2nd ed; Butterworth-Heinemann: London, 1994.

(10) Pratt, J. A.; McHugh, M. A. Supercritical-Fluid Fractionation of Poly(ethylene-*co*-acrylic acid). *J. Supercrit. Fluids* **1996**, *9*, 61−66.

(11) Dariva, C.; Oliveira, J. V.; Vale, M. G. R.; Caramão, E. B. Supercritical fluid extraction of high-ash Brazilian Coal. *Fuel* **1997**, *76*, 585−591.

(12) Sihvonen, M.; Järvenpää, E.; Hietaniemi, V.; Huopalahti, R. Advances in supercritical carbon dioxide technologies. *Trends Food Sci. Technol.* **1999**, *10*, 217−222.

(13) Camy, S.; Condoret, J. Dynamic modeling of a fractionation process for a liquid mixture using supercritical carbon dioxide. *Chem. Eng. Process.* **2001**, *40*, 499−509.

(14) Baysal, T.; Starmans, D. A. J. Supercritical carbon dioxide extraction of carvone and limonene from caraway seed. *J. Supercrit. Fluids* **1999**, *14*, 225−234.

(15) Gomes, M. F. T.; Antunes, O. A. C. Oxidation of Limonene Catalyzed by Mn^{III}(Salen)Cl.H_2O. *Catal. Lett.* **1996**, *38*, 133−134.

(16) Gomes, M. F. T.; Antunes, O. A. C. Autoxidation of limonene, α-pinene and β-pinene by dioxigen catalyzed by $Co(OAc)_2$/bromide. *J. Mol. Catal. A-Chem.* **1997**, *121*, 145−155.

(17) Akgün, M.; Akgün, N. A.; Dinçer, S. Phase behavior of essential oil components in supercritical carbon dioxide. *J. Supercrit. Fluids* **1999**, *15*, 117−125.

(18) Gamse, T.; Marr, R. High-pressure phase equilibria of de binary systems carvone-carbon dioxide and limonene-carbon dioxide at 30, 40 and 50 °C. *Fluid Phase Equilib.* **2000**, *171*, 165−174.

(19) Chang, C. M. J.; Chen, C. C. High-Pressure Densities and P−T−x−y Diagrams for Carbon Dioxide + Linalool and Cabon Dioxide + Limonene. *Fluid Phase Equilib.* **1999**, *163*, 119−126.

(20) Vieira de Melo, S. A. B.; Pallado, P.; Guarise, G. B.; Bertucco, A. High Pressure Vapor-Liquid Data for Binary and Ternary Systems formed by supercritical CO2 limonene and linalool. *Braz. J. Chem. Eng.* **1999**, *16*, 7.

(21) Iwai, Y.; Morotomi, T.; Koga, Y.; Arai, Y. High-Pressure Vapor Liquid Equilibria for Carbon Dioxide + Limonene. *J. Chem. Eng. Data* **1996**, *41*, 951.

(22) Byun, H. S.; Hasch, B. M.; McHugh, M. A. Phase behavior and modeling of systems CO_2-acetonitrile and CO_2-acrylic acid. *Fluid Phase Equilib.* **1996**, *115*, 179−192.

(23) Reighard, T. S.; Lee, S. T.; Olesik, S. V. Determination of methanol/CO_2 and acetonitrile/CO_2 vapor-liquid-phase equilibria using a variable-volume view-cell. *Fluid Phase Equilib.* **1996**, *123*, 215−230.

(24) Peng, D. Y.; Robinson, D. B. A new two-constant equation of state. *Ind. Eng. Chem. Fundam.* **1976**, *15*, 59.

(25) Reid, R. C.; Prausnitz, J. M.; Poling, B. E. *The Properties of Gases & Liquids*, 4th ed; McGraw-Hill: New York, 1988.

(26) Stuart, G. R.; Dariva, C.; Oliveira, J. V. High-pressure vapor-liquid equilibrium data for CO_2−Orange peel oil. *Braz. J. Chem. Eng.* **2000**, *17*, 181−189.

(27) Dariva, C.; Pinto, J. C.; Oliveira, J. V. High-pressure phase equilibria for polypropylene-hydrocarbon systems. *Ind. Eng. Chem. Res.* **2000**, *39*, 4627−4633.

(28) Dariva, C.; Pinto, J. C.; Tavares, F. W.; Oliveira, J. V. Phase behavior of polypropylene samples with hydrocarbon solvents at high pressures. *J. Appl. Pol. Sci.* **2001**, *81*, 3044−3055.

(29) Ndiyae, P. M.; Dariva, C.; Oliveira, J. V.; Tavares, F. W. Phase behavior of isotactic polypropylen/C4 solvents at high pressure. Experimental data and SAFT modeling. *J. Supercrit. Fluids* **2001**, *21*, 93−103.

(30) Dohrn, R.; Brunner, G. High-pressure fluid-phase equilibria: Experimental methods and systems investigated (1988−1993). *Fluid Phase Equilib.* **1995**, *120*, 213−282.

(31) Fornari, R. E.; Alessi, P.; Kikic, I. High-pressure fluid phase equilibria: Experimental methods and systems investigated (1983−1987). *Fluid Phase Equilib.* **1990**, *57*, 1−33.

(32) Cardozo-Filho, L. Modelagem da extração supercrítica de óleos essenciais, Ph.D. Thesis, FEA/Unicamp, Campinas, Brazil, 1999.

(33) Asselineau, L.; Bogdanic, G.; Vidal, J. A Versatile algorithm for calculating vapor-liquid equilibria. *Fluid Phase Equilib.* **1979**, *3*, 273−290.

Received for review August 5, 2002. Accepted November 19, 2002. The authors thank FAPERGS, CAPES, and CNPq for the technical and financial support of this research.

JE020150K